Influence of a simple fracture intersection on density-driven immiscible flow: Wetting vs. nonwetting flows

Sung-Hoon Ji,[1] Michael J. Nicholl,[2] Robert J. Glass,[3] and Kang-Kun Lee[1]

Received 21 March 2004; revised 26 May 2004; accepted 9 June 2004; published 27 July 2004.

[1] The influence of a single fracture intersection on density-driven immiscible flow is compared between wetting (water into air) and nonwetting (Trichloroethylene into water) flows. At low supply rates, the intersection acted as a hysteretic gate to pulsed flow of the wetting phase, but had minimal influence on nonwetting phase flow. For both cases, increasing the supply rate led to the formation of continuous fluid tendrils that crossed the intersection without interruption. The wetting experiment returned to pulsed flow as the supply rate was decreased, while the nonwetting experiment maintained a continuous flow structure. Results suggest a fundamental difference between wetting and nonwetting phase flows in fracture networks. *INDEX TERMS:* 1829 Hydrology: Groundwater hydrology; 1832 Hydrology: Groundwater transport; 1831 Hydrology: Groundwater quality; 1875 Hydrology: Unsaturated zone. **Citation:** Ji, S.-H., M. J. Nicholl, R. J. Glass, and K.-K. Lee (2004), Influence of a simple fracture intersection on density-driven immiscible flow: Wetting vs. nonwetting flows, *Geophys. Res. Lett.*, *31*, L14501, doi:10.1029/2004GL020045.

1. Introduction

[2] Recent experiments considering unsaturated flow in hydrophilic fracture networks have shown that capillary barriers formed at simple intersections between vertical and horizontal fractures can act to divert flow [*LaViolette et al.*, 2003], impose a temporal signal [*Glass et al.*, 2002; *Wood et al.*, 2002], and/or block lateral spreading [*Glass et al.*, 2003]. While not fully understood, this complex behavior clearly results from a sudden change in the relative importance of capillary forces that rises from the difference in void geometry between an intersection and the contributing fractures. Experiments to date have focused on the density-driven flow of a wetting phase (i.e., water into an otherwise air-filled hydrophilic system). The influence of fracture intersections has yet to be considered for the density-driven flow of a nonwetting phase, such as would occur during the invasion of a water-saturated fracture network by a Dense Nonaqueous Phase Liquid (DNAPL).

[3] Here we present a first experiment designed to explore the differences between wetting and nonwetting flows at a simple intersection between vertical and horizontal fractures of equal aperture ($\sim$371 μm). Density-driven flow of a wetting phase was considered by supplying water to an air-filled (dry) system; for nonwetting phase flow, we submerged the same intersection in water, then introduced Trichloroethylene (TCE) as a DNAPL. In both cases we varied the supply rate across $\sim$3 orders of magnitude, first increasing the supply rate and then decreasing it. At all supply rates, the influence of this simple intersection differed substantially between the wetting and nonwetting experiments. We expect that these differences would be exacerbated at the network scale, leading to fundamentally different spatial and temporal behavior between wetting and nonwetting flows.

2. Experimental Design

[4] A two-dimensional analog intersection was fabricated by inducing controlled breaks in a 25.4 $\times$ 25.4 $\times$ 1.9 cm glass plate (Figure 1a). The fractured plate was then supported by clamping it between two unbroken glass plates of the same size (Figure 1b). The fractures composing our test intersection (center of Figure 1a) were held open by inserting three pieces of 371 μm diameter wire into each fracture segment. Each wire was bent to a 90° angle. The short leg of the wire ($\sim$0.1 cm) was inserted into the fracture aperture, while the longer leg ($\sim$1–2 cm) was taped to the face of the glass plate in order to hold the wire in place (see Figures 2–4). The wires holding the fractures open were placed such that they did not influence behavior at the intersection, which is our principal area of interest. However, as seen in Figures 3b and 3d, the wires did perturb flow paths within the fracture planes.

[5] The other fractures in the system were designed to act as boundaries. Vertical fractures to the left and right of the test intersection were established as capillary barriers to the flowing phase; 650 μm wire was inserted to block wetting phase flow and 295 μm wire for nonwetting phase flow. To facilitate entry by the flowing phase, the horizontal fracture below the test intersection was held open with 650 μm wire for nonwetting phase flow and 295 μm wire for wetting phase flow. Finally, we inserted boundary spacers between the fractured plate and the supporting plates (Figure 1b) to impose capillary barriers to the flowing phase. This gap was set at $\sim$1100 μm for wetting phase flow, and $\sim$80 μm for nonwetting phase flow.

[6] A syringe pump was used to inject the flowing phase (water or TCE) into the vertical fracture at a location 7.6 cm above the intersection (Figure 1a). The non-flowing phase (air or water) was allowed to escape freely through all fracture edges. Wetting phase flow was considered under initially dry (air-filled) conditions. For nonwetting phase flow, we submerged the model in clear water to a depth of

[1]School of Earth and Environmental Sciences, Seoul National University, Seoul, Korea.
[2]Geoscience Department, University of Nevada, Las Vegas, Nevada, USA.
[3]Flow Visualization and Processes Laboratory, Sandia National Laboratories, Albuquerque, New Mexico, USA.

Copyright 2004 by the American Geophysical Union.
0094-8276/04/2004GL020045$05.00

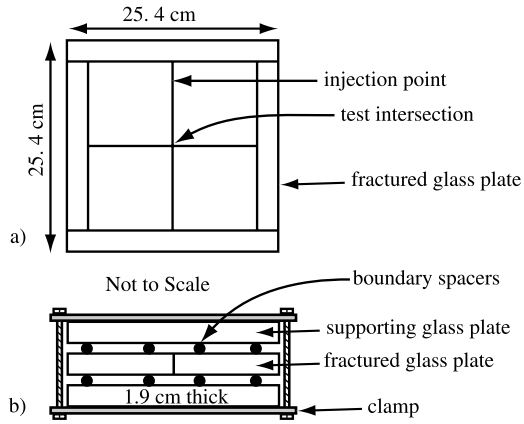

Figure 1. Fracture intersection model. (a) Side view of the fractured plate. Individual fractures were generated by electrically heating a strip of Nichrome™ wire pressed against the glass [*Glass et al.*, 2003]. The resulting fractures are slightly curvilinear, and have nearly smooth surfaces with a faint conchoidal texture. Note that the high contrast in refractive index between air and glass overemphasizes the conchoidal texture of the fracture surfaces (compare Figures 2 and 4). (b) Horizontal cross-section showing the supporting plates, clamps, and boundary spacers.

~5.1 cm above the injection point, making sure to eliminate all entrapped air from within the fractures and test intersection. In both cases, the flowing phase was dyed to improve visibility; for water, we added 1.0 g/l of FD&C Blue #1, while 0.9 g/l of Oil-Red-O was added to the TCE (see Table 1 for fluid properties). Prior to and between experiments, surfaces of the analog fractures were cleaned thoroughly to restore a uniform contact angle ($\alpha \sim 5°$ for water-air, $\alpha \sim 160°$ for TCE-water).

3. Results

[7] At the start of each experiment the fracture network was filled with a single fluid phase (air or water). Then we applied the flowing phase (water or TCE) in a series of contiguous steps; first increasing the supply rate (0.012, 0.10, 0.50, 1.00, 5.00, and 10.00 ml/min) and then decreasing it along the same sequence. At each step, the supply rate was held constant for the longer of 5 minutes or 2 ml injection volume. We chose this range of supply rates to vary the influence of viscous forces upwards from negligible. From the cubic law [e.g., *Bird et al.*, 1960] and linear stability theory [e.g., *Saffman and Taylor*, 1958], we would expect viscous stabilized displacement for both cases (water-air and TCE-water) at supply rates of ~50–60 ml/min, and selected our maximum supply rate (10 ml/min) to be of similar order.

3.1. Wetting Invasion

[8] Initial injection of water into the air-filled system at 0.012 ml/min produced a slow sequence of small water blobs (~0.7 × 0.2 cm) in the upper vertical fracture. Each blob exhibited a bulbous head and a narrow tail [see also *Wood et al.*, 2002]. The first fluid blob established a wetted pathway to the intersection that was followed by subsequent flow. As observed elsewhere [*Wood et al.*, 2002; *Glass et al.*, 2003], water pooled above the capillary barrier formed by the intersection (Figure 2). The growing pool was constrained laterally by capillary barriers at the fracture edges, while the top of the pool exhibited a curvilinear surface within the fracture plane. Upon reaching a height of

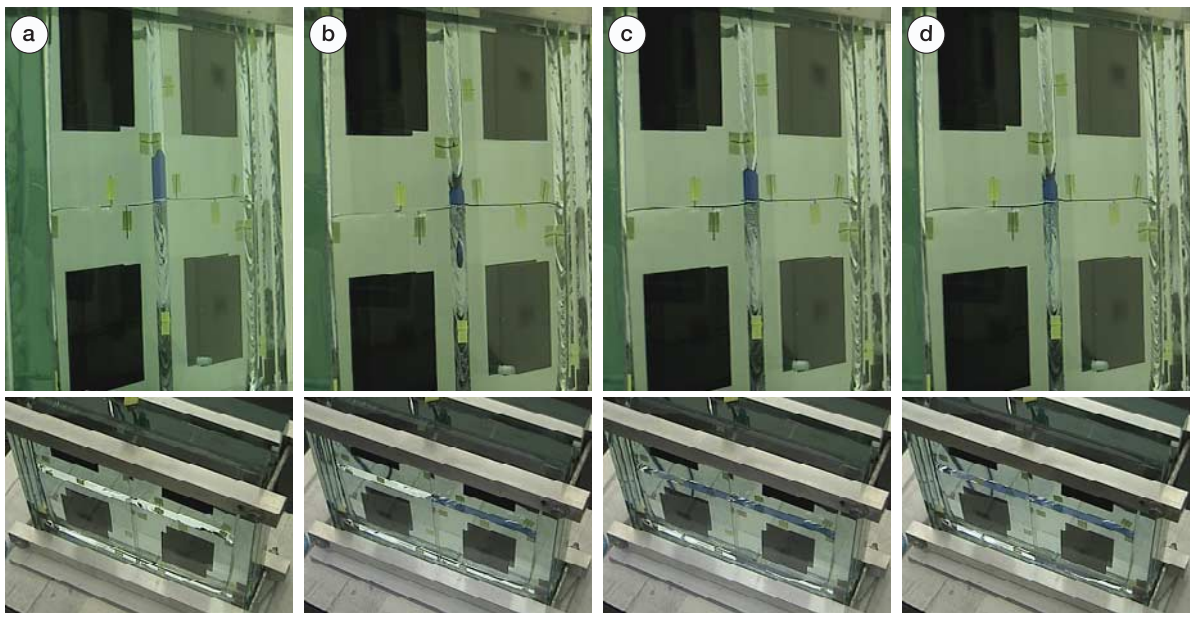

Figure 2. Initial invasion of water (blue) into the air-filled intersection at a supply rate of 0.012 ml/min. The large black squares are ~1100 μm boundary spacers (Figure 1b). Upper view is looking sideways into the vertical fracture, while the lower view looks downwards into the horizontal fracture. (a) Maximum pool height prior to entry into the right-hand fracture. (b) Release of a fluid blob as water first enters the left-hand fracture. Maximum (c) and minimum (d) pool heights during the regular fill and drain cycle.

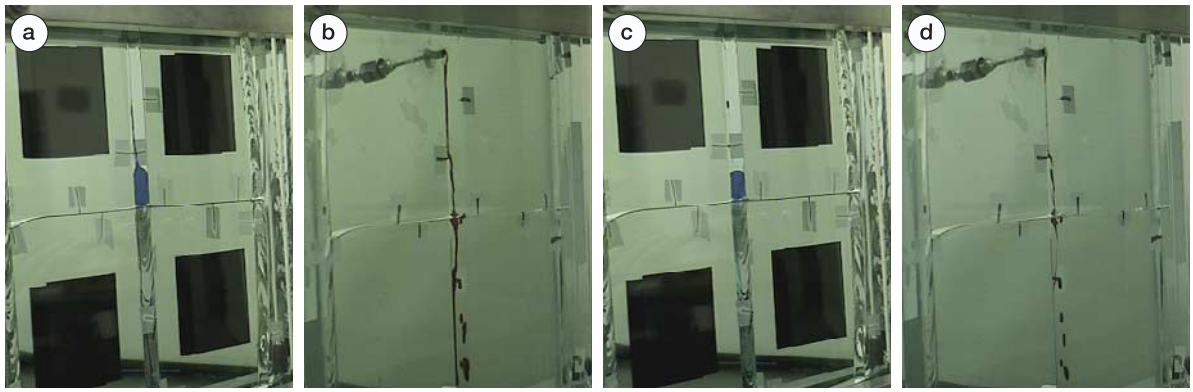

Figure 3. Side view of fluid tendrils formed at a supply rate of 10 ml/min for (a) wetting and (b) nonwetting phase flow. Fluid structures after reducing the supply rate to 0.012 ml/min for (c) wetting and (d) nonwetting phase flow.

2.18 cm above the intersection (Figure 2a) the pool invaded the right-hand horizontal fracture and partially drained. Pool height rose after the right-hand fracture was full, then fell as water entered into the left-hand fracture (Figure 2b). At the same time (59 minutes after starting flow), a single water blob was released into the lower vertical fracture.

[9] Storage in the left-hand fracture filled ~134 minutes after starting flow. The intersection then developed a regular fill and drain cycle. In each cycle, pool height rose to 1.42 cm (Figure 2c), breaching the capillary barrier and releasing fluid into the lower vertical fracture as a discrete blob. Before the blob separates, it applies sufficient tension to lower pool height to 0.87 cm (Figure 2d). The maximum pool height during each cycle (1.42 cm, Figure 2c) is less than that required for initial invasion of the intersection (2.18 cm, Figure 2a). The observed diversion of flow into the horizontal fractures is consistent with other experiments [e.g., *Wood et al.*, 2002; *Glass et al.*, 2003]. Selection of the initial diversion direction (left vs. right) apparently results from local intersection geometry. Note that unlike the experiments of *Wood et al.* [2002] in a geometrically similar intersection composed of cut limestone blocks, water storage in the horizontal fractures was static, and did not participate in the fill and drain cycle.

[10] Flow above the intersection transitioned from discrete blobs to a continuous tendril when the supply rate was increased to 0.1 ml/min. The intersection continued to act as a dynamic barrier, releasing large fluid blobs at regular intervals. Pool height fell from a maximum of 1.33 cm to a minimum of 0.87 cm when a blob was released. At supply rates of 0.5 ml/min and higher, tendrils also formed below the intersection, eliminating pulsation. The tendrils widened as the supply rate was stepped up to 10 ml/min (Figure 3a), however the static pool height (~1.03 cm) remained intermediate to that observed during pulsing regimes. The fluid tendrils narrowed as the supply rate was stepped down, with pulsed flow returning below the intersection at 0.1 ml/min, and above at 0.012 ml/min (Figure 3c). Behavior as flow was stepped down was not completely symmetric with the increasing cycle, as the range of pool heights during the fill and drain cycle at 0.012 ml/min narrowed to a maximum of 1.29 cm and a minimum of 0.88 cm. In contrast to *Wood et al.* [2002], tendrils and blob flow maintained a single pathway throughout the experiment.

3.2. Nonwetting Invasion

[11] Initial injection of TCE into the water-filled system at 0.012 ml/min produced a sequence of medium-sized (~1.1 × 0.6 cm) TCE blobs in the upper vertical fracture (Figure 4). Blobs formed with a bulbous head and narrow tail, but quickly became rounded during advancement. The first blob entered the intersection and stopped (Figure 4a) because the fractures exiting the intersection formed capillary barriers (decreasing aperture). Additional blobs reaching the intersection led to upwards growth and limited

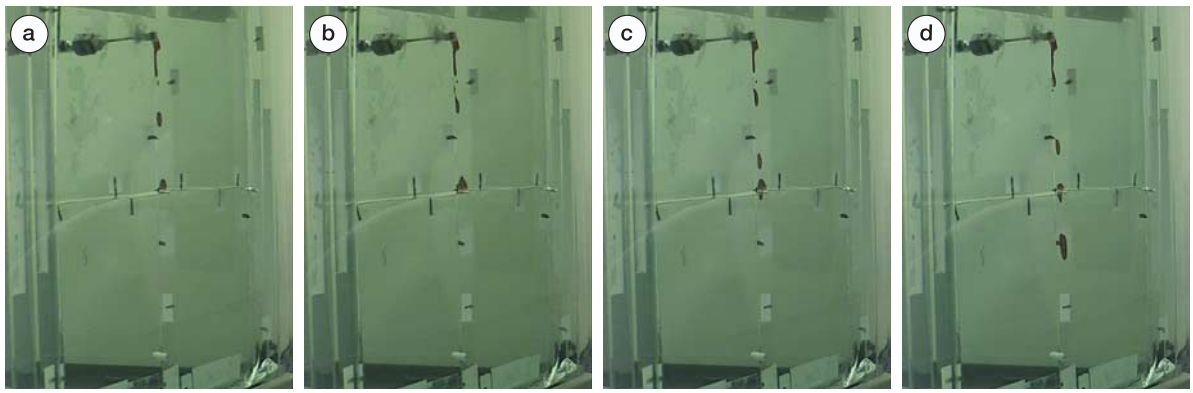

Figure 4. Sequence showing initial invasion of TCE (red) into a water saturated fracture intersection at a supply rate of 0.012 ml/min; view is from the side.

Table 1. Physical Properties of Experimental Fluids

Fluid	Density (g/ml)	Viscosity (cp at 25°C)	Interfacial Tension (mN/m)
Water[a]	0.998	1.000	NA
Air[a]	0.001	0.018	73
TCE[b]	1.469	0.575	27

[a]From *Weast* [1985].
[b]From *Glass et al.* [2000].

lateral spreading that was constrained by one fracture edge, but not the other (Figure 4b). The TCE pool began to invade the lower vertical fracture when it reached a maximum height of 0.62 cm above the intersection (Figure 4c). Continued addition of fluid led to growth of a hanging fluid column beneath the intersection and the release of a large fluid blob (Figure 4d).

[12] The first release of pooled TCE from the intersection occurred 1.5 minutes after starting the experiment. Afterwards, flow rapidly settled into a steady regime; shortly after a blob of TCE arrived at the intersection, a blob of similar size was released from below. Pool height dropped as each blob was released, however the upper edge of the pool never entered the intersection. Similarly, the bottom of the pool never retreated into the intersection. The exiting blob always separated from the pool within the fracture itself, and at a distance below the intersection. As a result, a pool of TCE remained pinned across the intersection, acting as a capillary bridge between the upper and lower vertical fractures. The persistence of this bridge precluded TCE entry into either of the horizontal fractures.

[13] Flow above the intersection transitioned from discrete blobs to a pulsing tendril when the supply rate was increased to 0.50 ml/min; TCE release below the intersection occurred as large blobs. The tendril above the intersection stabilized at a supply rate of 1.0 ml/min, and a stable tendril formed below the intersection at 5.0 ml/min. Tendril width increased to a maximum at 10.0 ml/min (Figure 3b), then narrowed, but did not snap as the supply rate was stepped down to 0.012 ml/min (Figure 3d). At some locations, the tendril detached from one fracture surface as it shrank to a diameter of less than the fracture aperture. This dramatic shrinkage was localized and led to a pool and thread structure within the fracture plane. Pathways changed somewhat during blob flow, but remained constant for the tendrils. Throughout the sequence of increasing supply rates the pool trapped across the intersection decreased in size, but remained in place. This smaller size pool was retained as flow was stepped down.

4. Summary and Discussion

[14] Our experiments showed a substantial difference between wetting and nonwetting flows at a simple intersection between horizontal and vertical fractures of equal aperture ($\sim$371 μm). At low supply rates, the intersection acted as a hysteretic gate to flow of the wetting phase. Water accumulated above the intersection, which formed a capillary barrier. The integrated volume was then released at regular intervals. Conversely, the intersection provided little hindrance to flow of the nonwetting phase. A small pool of TCE remained pinned across the intersection, acting as a capillary bridge. For the wetting phase experiment, the capillary barrier initially diverted flow into the horizontal fractures, substantially delaying downwards migration. In contrast, the TCE did not enter either horizontal fracture, and migrated downwards rapidly. For both wetting and nonwetting flows, increasing the supply rate led to the formation of continuous fluid tendrils that crossed the intersection without interruption. The wetting experiment returned to pulsed flow as the supply rate was decreased, while the nonwetting experiment maintained a fully connected flow structure.

[15] Projection of our results to a regular network of equal aperture vertical and horizontal fractures suggests substantial differences between wetting and nonwetting flows. The absence of entry into the horizontal fractures by the nonwetting phase would preclude the following phenomena observed for wetting phase flow: macroscopic flow convergence [*LaViolette et al.*, 2003], pathway switching [*Glass et al.*, 2002, 2003], and temporal fluctuations in outflow over a range of scales [*Glass et al.*, 2002]. Instead, we expect that the nonwetting phase would move rapidly along narrow pathways through the vertical fractures, establishing small pools at each intersection along the way. The persistence of continuous tendrils would act to provide high conductivity pathways through the system, even with a declining source term. The resulting focused transport pathways would be highly difficult to locate and remediate.

[16] **Acknowledgments.** This study was supported by U.S. Department of Energy's Environmental Management Science Program under contact DE-AC04-94AL85000 at Sandia National Laboratories and DE-FG07-02ER63499 at the University of Idaho, the BK 21 project of the Korean Government, and AEBRC of POSTECH. We would also like to acknowledge assistance from L. Orear in fabricating the experimental apparatus.

References

Bird, R. B., W. E. Stewart, and E. N. Lightfoot (1960), *Transport Phenomena*, 780 pp., John Wiley, Hoboken, N. J.

Glass, R. J., S. H. Conrad, and W. Peplinski (2000), Gravity destabilized nonwetting phase invasion in macroheterogeneous porous media: Experimental observations of invasion dynamics and scale analysis, *Water Resour. Res.*, *36*(11), 3121–3138.

Glass, R. J., M. J. Nicholl, S. E. Pringle, and T. R. Wood (2002), Unsaturated flow through a fracture-matrix network: Dynamic preferential pathways in mesoscale laboratory experiments, *Water Resour. Res.*, *38*(12), 1281, doi:10.1029/2001WR001002.

Glass, R. J., M. J. Nicholl, H. Rajaram, and T. R. Wood (2003), Unsaturated flow through fracture networks: Evolution of liquid phase structure, dynamics, and the critical importance of fracture intersections, *Water Resour. Res.*, *39*(12), 1352, doi:10.1029/2003WR002015.

LaViolette, R. A., R. J. Glass, T. R. Wood et al. (2003), Convergent flow observed in a laboratory-scale unsaturated fractured system, *Geophys. Res. Lett.*, *30*(2), 1083, doi:10.1029/2002GL015775.

Saffman, P. G., and G. I. Taylor (1958), The penetration of a fluid into a porous medium or Hele-Shaw cell containing a more viscous liquid, *Proc. R. Soc. London, Ser. A*, *245*, 312–331.

Weast, R. C. (Ed.) (1985), *CRC Handbook of Chemistry and Physics*, 66th ed., CRC Press, Boca Raton, Fla.

Wood, T. R., M. J. Nicholl, and R. J. Glass (2002), Fracture intersections as integrators for unsaturated flow, *Geophys. Res. Lett.*, *29*(24), 2191, doi:10.1029/2002GL015551.

R. J. Glass, Flow Visualization and Processes Laboratory, Sandia National Laboratories, P.O. Box 5800, Albuquerque, NM 87185-1137, USA. (rjglass@sandia.gov)

S.-H. Ji and K.-K. Lee, School of Earth and Environmental Sciences, Seoul National University, Seoul 151-747, Korea. (ji0511@snu.ac.kr; kklee@snu.ac.kr)

M. J. Nicholl, Geoscience Department, University of Nevada, 4505 Maryland Parkway, Las Vegas, NV 89122, USA. (michael.nicholl@ccmail.nevada.edu)